Simple empirical $E1$ and $M1$ strength functions for practical applications

S. Goriely[1] and V. Plujko[2]
[1]*Institut d'Astronomie et d'Astrophysique, Université Libre de Bruxelles, CP-226, 1050 Brussels, Belgium*
[2]*Taras Shevchenko National University, Kiev 01601, Ukraine*

(Received 18 October 2018; published 7 January 2019; corrected 5 February 2019)

Valuable theoretical predictions of nuclear dipole excitations in the whole chart are of great interest for different nuclear applications, including, in particular, nuclear astrophysics. Here on the basis of experimental and theoretical information on the $E1$ and $M1$ strength functions, inspired both from axially deformed quasiparticle random-phase approximation and shell-model calculations, we derive simple expressions to determine systematically the dipole strength in order to update former prescriptions with a special emphasis on new expressions for the $M1$ spin-flip and scissors modes. We compare our final prediction of the $E1$ and $M1$ strengths with available experimental data at low energies and show that a relatively good agreement is obtained. Its impact on the total radiative width as well as radiative neutron capture cross sections is also discussed. The new expressions are believed to represent an improvement with respect to the analytical systematics proposed in the past and used traditionally in reaction codes, such as the recommended RIPL-3 prescriptions.

DOI: 10.1103/PhysRevC.99.014303

I. INTRODUCTION

Radiative neutron capture cross sections play a key role in almost all nuclear applications. Despite a huge effort to measure such radiative neutron capture cross sections, theoretical predictions are required to fill the gaps, both for nuclei for which measurements are not feasible at the present time, in particular, for unstable targets, and for energies that cannot be reached in the laboratory. Some applications, such as nuclear astrophysics, also require the determination of radiative neutron capture cross sections for a large number of exotic neutron-rich nuclei [1]. In this case, large-scale calculations need to be performed on the basis of sound and accurate models to ensure a reliable extrapolation far away from the experimentally known region.

The neutron capture rates are commonly evaluated within the framework of the statistical model of Hauser-Feshbach, although the direct capture contribution plays an important role for very exotic nuclei [2]. The fundamental assumption of the Hauser-Feshbach model is that the capture goes through the intermediary formation of a compound nucleus in thermodynamic equilibrium. In this approach, the (n,γ) cross section strongly depends on the electromagnetic interaction, i.e., the photon deexcitation probability. It is well known that the photon strength function is dominated by the dipole contribution. The various multipolarities of the γ-ray strength function are traditionally modeled by the phenomenological Lorentzian approximation or some of its energy-dependent width variants [3].

The reliability of the γ-ray strength predictions can be greatly improved by the use of microscopic or semimicroscopic models. Such an effort can be found in Refs. [4–9] where a complete set of $E1$ and $M1$ γ-ray strength functions was derived from mean field plus quasiparticle random-phase approximation (QRPA) calculations. When compared with experimental data and considered for practical applications, all mean-field plus QRPA calculations need however some phenomenological corrections. These include a broadening of the QRPA strength to take the neglected damping of collective motions into account as well as a shift of the strength to lower energies due to the contribution beyond the one-particle–one-hole excitations and the interaction between the single-particle and low-lying collective phonon degrees of freedom [10–17]. In addition, most of the mean-field plus QRPA calculations assume spherical symmetries so that phenomenological corrections need to be included in a way or another in order to properly describe the splitting of the giant dipole resonance in deformed nuclei. State-of-the-art calculations including effects beyond the one-particle–one-hole excitations and phonon coupling are now available [10–17], but they remain computerwise intractable for large-scale applications.

Despite the availability of such tabulated $E1$ and $M1$ strengths, many nuclear reaction codes still make use of simple analytical formulas that present the advantage of being easily tuned on experimental data but also adjustable to reproduce measured cross sections. Such expressions have been recommended by the latest Reference Input Parameter Library (RIPL-3) [3] and are usually described by a Lorentzian-type function or some variants of it [3,18]. One of the most commonly used expression corresponds to the standard Lorentzian (SLO) [19,20] or the generalized Lorentzian (GLO) [18] which differs from the SLO by including an energy-dependent width. Although the $E1$ strength has been widely studied [see, for example, Refs. [3,18,21,22] and references therein], less effort has been devoted to the parametrization of the $M1$ strength function for practical applications. The most commonly used formula is an SLO expression describing the spin-flip (sf) mode only [18] that neglects the low-energy $M1$ mode for deformed nuclei (the so-called scissors mode). Only a few works [23–25] proposed a systematic phenomenological

 ©2019 American Physical Society

description of the low-energy scissors mode. In addition, such formulas only describe the photoabsorption, whereas it is now well accepted that the deexcitation strength function may differ from the photoabsorption one, especially at low photon energies. In particular, a nonzero limit of the dipole strength has been observed experimentally [26,27] and confirmed by shell-model (SM) calculations [28–33]. For this reason, the predictions have to be complemented with a zero limit that is missing in the present $M1$ SLO description.

In the present paper, we propose simple Lorentzian-type expressions to describe $E1$ and $M1$ strength functions with a special emphasis on new expressions for both the spin-flip and the scissors (sc) mode components of the $M1$ strength. These formulas, hereafter referred to as SMLO for simple modified $E1$ Lorentzian and simple $M1$ Lorentzian, are explained in Secs. II and III for the $E1$ and $M1$ modes, respectively. The expressions are kept as simple as possible, still trying to capture as much as possible systematics found in more microscopic approaches, such as the QRPA and SM predictions. Average resonance capture (ARC) data as well as nuclear resonance fluorescence (NRF) data are used to test or tune our new prescriptions. In Sec. IV, we compare our SMLO predictions with experimental data that are sensitive to the total dipole $E1 + M1$ strength. These concern the data obtained through the Oslo method as well as the average radiative width $\langle \Gamma_\gamma \rangle$ and neutron capture cross sections. Conclusions are finally drawn in Sec. V.

II. THE $E1$ PHOTOABSORPTION STRENGTH

For the $E1$ photon strength function of cold and heated nuclei, we consider here the SMLO model that provides a rather simple expression [22],

$$\overleftarrow{f_{E1}} = \frac{1}{3\pi^2\hbar^2c^2}\frac{1}{1-\exp(\varepsilon_\gamma/T)}\sigma_{\rm TRK} \times \frac{2}{\pi}\sum_{j=1}^{j_m} s_{r,j}\frac{\varepsilon_\gamma\,\Gamma_j(\varepsilon_\gamma,T)}{\left(\varepsilon_\gamma^2-E_{r,j}^2\right)^2+\varepsilon_\gamma^2\Gamma_j(\varepsilon_\gamma,T)^2}, \quad (1)$$

where T denotes to the temperature of the heated nucleus, j_m denotes the number of normal vibration modes of the giant dipole resonance (GDR) excitation ($j_m = 1$ for spherical nuclei and 2 for axially deformed ones), and $\sigma_{\rm TRK}$ is the Thomas-Reiche-Kuhn (TRK) sum rule given by

$$\sigma_{\rm TRK} = 60\frac{NZ}{A} = 15A(1-I^2)\ ({\rm mb\,MeV}), \quad (2)$$

where $I = (N-Z)/(N+Z)$ is the neutron-proton asymmetry factor. The Lorentzian function in Eq. (1) is characterized by GDR parameters corresponding to the peak energy $E_{r,j}$, the width at half maximum Γ_j, and the possible deviation of the peak cross section from the TRK sum rule $s_{r,j}$. More details on these quantities are given below.

The SMLO width, related to the relaxation mechanism the giant vibration j mode, is taken to be energy and temperature dependent as

$$\Gamma_j(\varepsilon_\gamma,T) = \frac{\Gamma_{r,j}}{E_{r,j}}\left(\varepsilon_\gamma + \frac{4\pi^2}{E_{r,j}}T^2\right), \quad (3)$$

where the linear dependence on the energy ε_γ comes from the inverse ε_γ dependence of the average squared matrix element in the transitions of the one-particle–one-hole states to two-particles–two-hole states [3]. The quadratic temperature dependence in Eq. (3) originates from the Fermi-liquid theory.

The GDR resonance energies of the j mode are taken such that $E_{r,j=1} < E_{r,j=2}$, at least, for deformed nuclei (for spherical nuclei, $E_{r,j=1} = E_{r,j=2}$). These energies are connected to the energies E_a and E_b of the vibrations along and perpendicular to the symmetry axis (note that for prolate nuclei, we take $E_{r,1} = E_a$ and $E_{r,2} = E_b$, whereas for oblate ones, $E_{r,1} = E_b$ and $E_{r,2} = E_a$). Finally, the $s_{r,j}$ factor gives the weight of the j mode with respect to the TRK sum rule.

Whenever experimental photoabsorption data in the vicinity of the GDR are available, the GDR parameters $E_{r,j}$, $\Gamma_{r,j}$, and $s_{r,j}$ can be adjusted. A compilation of such data can be found in Ref. [22]. However, when no data exist, some systematics need to be provided. Such a systematic was obtained by a least-squares fit to the recommended experimental GDR parameters in spherical nuclei as well as deformed nuclei in the $150 < A < 190$ and $220 < A < 253$ ranges where in good approximation deformed nuclei can be considered as axially deformed. The following expression was adopted for the centroid energy E_r of the GDR:

$$E_r = e_1(1-I^2)^{1/2}\frac{A^{-1/3}}{(1+e_2A^{-1/3})^{1/2}}, \quad (4)$$

where $e_1 = 128.0 \pm 0.9$ MeV and $e_2 = 8.5 \pm 0.2$. Equation (4) corresponds to a good approximation of the eigenenergy of the GDR vibration within the hydrodynamical liquid drop model [34] also in link with sum rule prescriptions [35–37]. For deformed nuclei, we assume the equiprobability of the normal mode excitations and the twofold degeneracy of the giant collective vibration perpendicular to the axis of symmetry. In this case, the centroid energy can be expressed as $E_r = (E_a + 2E_b)/3$, and the energies E_a and E_b along the two ellipsoid semiaxes can be approximated as

$$E_a = \frac{3E_r}{1+2D}, \quad (5)$$

$$E_b = DE_a, \quad (6)$$

where $D = 0.911a/b + 0.089$ can be determined from the ratio of the ellipsoid semiaxis lengths $a/b = (1+\alpha_2)/(1-\alpha_2/2)$, which, in turn, is a function of the quadrupole deformation β_2 since $\alpha_2 = \sqrt{5/4\pi}\,\beta_2$.

Slight deviations from the TRK sum rule is known from experimental photoabsorption data; for this reason, the weights of the j mode is estimated assuming that $s_\Sigma = \sum_j s_j = 1.2$, i.e., $s_1 = s_\Sigma/3$, $s_2 = 2s_\Sigma/3$ for prolate nuclei and $s_1 = 2s_\Sigma/3$, $s_2 = s_\Sigma/3$ for oblate nuclei.

As far as the GDR width is concerned, it can be estimated from a simple power-law expression $\Gamma_{r,j} = cE_{r,j}^d$ with $c = 0.42 \pm 0.05$ MeV and $d = 0.90 \pm 0.04$. More details on the model and the adjustment can be found in Refs. [21,22,38]. Note that the high-energy quasideuteron contribution, i.e., the photoabsorption cross section on a neutron-proton pair is not included here but can be found in Ref. [22].

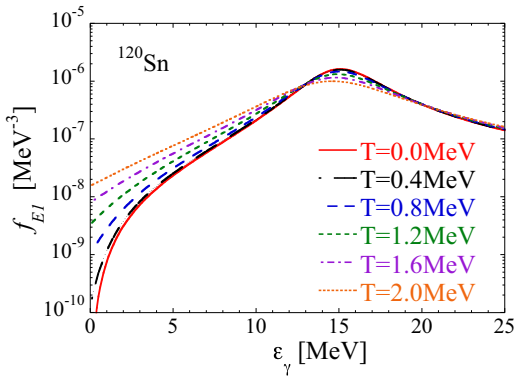

FIG. 1. T dependence of the SMLO $E1$ strength function of ^{120}Sn as a function of the photon energy.

Finally, the temperature T can be derived from the excitation energy U using a simple Fermi gas expression. Since the temperature entering Eq. (1) corresponds to the temperature of the final state, it reads $T = \sqrt{(U - \varepsilon_\gamma)/\tilde{a}}$ where the level-density parameter $\tilde{a} = A/10$ MeV^{-1} is adopted. The T dependence of the SMLO $E1$ strength and its impact at low photon energies are illustrated in Fig. 1 for ^{120}Sn.

Up to now, the SMLO model has been essentially adjusted on photoabsorption data and out of it some systematics deduced. We compare in Fig. 2 the predicted $E1$ strengths with ARC data at energies around 6 to 7 MeV [39]. A rather satisfactory agreement is found bringing additional confidence to the low-energy extrapolation of the SMLO $E1$ strength. More comparisons with experimental photoabsorption data can be found in Ref. [22], and an additional one will be discussed in Sec. IV.

III. THE $M1$ PHOTOABSORPTION STRENGTH

Although much effort has been devoted in the past to the modeling of the $E1$ strength, only a reduced number of systematics exists regarding the $M1$ contribution. The $M1$ strength has been described essentially through a SLO expression describing the spin-flip mode [3,18]. Important progress has been made for the past decade in describing microscopically the $M1$ strength either within mean-field plus QRPA methods or the SM (for a review, see Ref. [40]). Such work can be used to help us to construct empirical expressions. In particular, recent axially deformed Hartree-Fock-Bogolyubov (HFB) plus QRPA calculations based on the Gogny D1M interaction, hereafter referred to as D1M + QRPA [7–9] can help us to build new empirical $M1$ strength functions. To do so, we have chosen to adopt simple SLO expressions for both the low-energy sc mode and the sf components of the $M1$ strength function, i.e.,

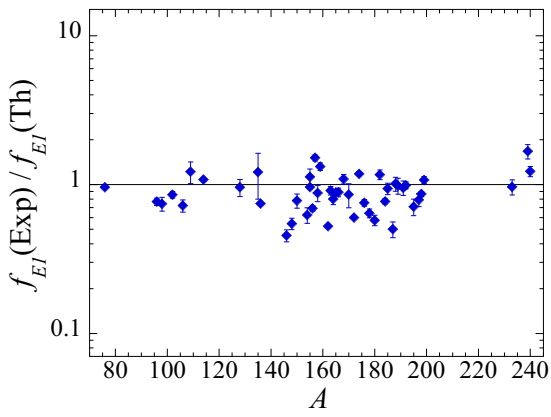

FIG. 2. Comparison between the experimental $E1$ strengths from ARC data [39] with the T-dependent SMLO predictions for the 47 nuclei recently reanalyzed.

$$\overrightarrow{f_{M1}}(\varepsilon_\gamma) = \frac{1}{3\pi^2\hbar^2c^2}\sigma_{\rm sc}\frac{\varepsilon_\gamma\Gamma_{\rm sc}^2}{\left(\varepsilon_\gamma^2 - E_{\rm sc}^2\right)^2 + \varepsilon_\gamma^2\Gamma_{\rm sc}^2} + \frac{1}{3\pi^2\hbar^2c^2}\sigma_{\rm sf}\frac{\varepsilon_\gamma\Gamma_{\rm sf}^2}{\left(\varepsilon_\gamma^2 - E_{\rm sf}^2\right)^2 + \varepsilon_\gamma^2\Gamma_{\rm sf}^2}, \quad (7)$$

where $\sigma_i = f_i E_i$ is the peak cross section, E_i is the the energy at the peak, and Γ_i is the the width at half maximum for both the spin-flip mode ($i = $ sf) or the scissors mode ($i = $ sc).

Inspired from the mass and deformation dependences of the D1M + QRPA strengths, the energy and width of the Lorentzian-type function can be determined in a simple manner. As far as the amplitude of the strength σ_i is concerned, the D1M + QRPA calculations predict that, globally, the centroid energy decreases as $A^{-1/6}$ [Fig. 3(a)] and the spin-flip peak strength $f_{\rm sf}$ increases linearly with A [Fig. 3(b)] so that the peak cross section $\sigma_{\rm sf}$ scales like $A^{5/6}$. For the scissors mode, present only in deformed nuclei, the centroid energy remains rather constant around 3 MeV decreasing as $A^{-1/10}$ [Fig. 4(a)], whereas the peak strength $f_{\rm sc}$ is found to be globally proportional to A and to the quadrupole deformation parameter β_2 [Fig. 4(b)]. Note that some neutron shell structures can be observed in the D1M + QRPA predictions of the spin-flip and scissors modes that cannot be described by a simple analytical expression. We have chosen to restrict ourselves to simple expressions. The amplitude of the strength can, in turn, be tuned by comparing our $M1$ prescriptions [Eq. (7)] with existing data, namely, the ARC data [39] for the spin-flip mode and the NRF experiments in the rare-earth region for the scissors mode (see below).

When considering the deexcitation strength function, deviations from the photoabsorption strength can be expected, especially for γ-ray energies approaching the zero limit. In particular, SM calculations [28–33] predict an exponential increase in the $M1$ deexcitation strength function at decreasing energies approaching zero. This so-called upbend of the strength function observed experimentally [26,27] has therefore been assumed to be of $M1$ nature, although no experimental evidence exists for the moment. Therefore, when dealing with the deexcitation $M1$ strength function, a zero-energy limit as determined in Ref. [9] can be added to the photoabsorption expression, leading to

$$\overleftarrow{f_{M1}}(\varepsilon_\gamma) = \overrightarrow{f_{M1}}(\varepsilon_\gamma) + C\ \exp(-\eta\varepsilon_\gamma), \quad (8)$$

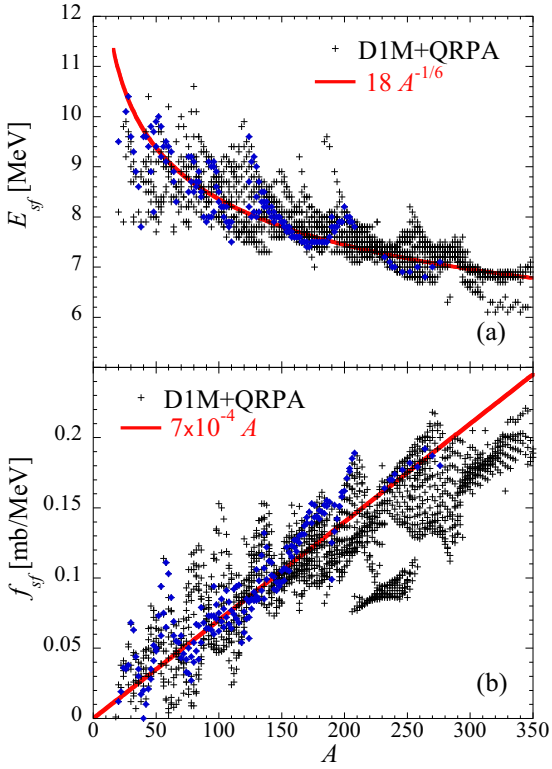

FIG. 3. (a) Peak energy of the spin-flip resonance obtained within the D1M + QRPA approach [9] as a function of the atomic mass number for some 2000 even-even nuclei with $8 \leqslant Z \leqslant 110$ lying between the proton and the neutron drip lines. (b) The same for the peak strength $f_{\rm sf}$. The red line corresponds to the simple analytical expressions adopted in the present paper. The blue diamonds correspond to the D1M + QRPA values for stable nuclei and long-lived actinides.

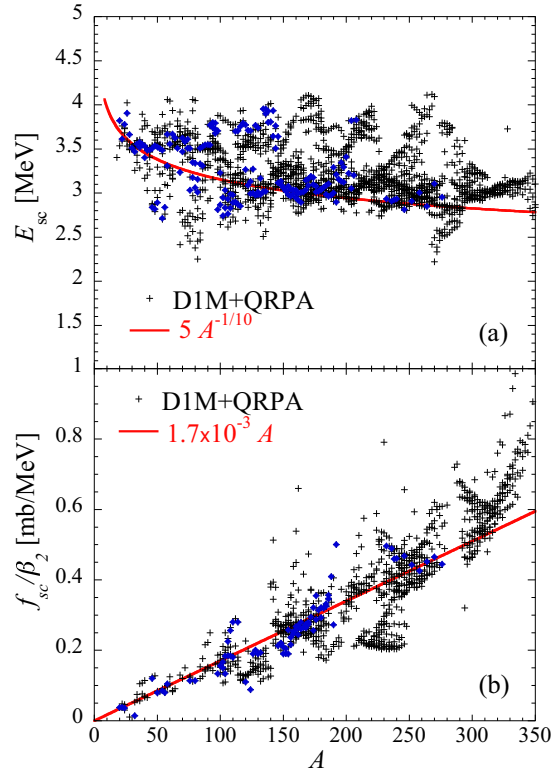

FIG. 4. (a) The same as Fig. 3 for the scissors mode strength below 4.5 MeV. Only deformed nuclei for which the D1M + QRPA scissors mode is non-negligible are shown. (b) The same for the peak strength of the scissors mode divided by D1M β_2 [41]. The blue diamonds correspond to the D1M + QRPA values for stable nuclei and long-lived actinides.

where the parameter C is now taken to be deformation dependent as inferred from SM calculations [31–33,42] and a recent analysis of experimental multistep cascade spectra [43].

Finally, we adopt the following parameters for the three $M1$ modes, i.e., for

(1) the spin-flip resonance: $\sigma_{\rm sf} = 0.03A^{5/6}$ mb, $E_{\rm sf} = 18A^{-1/6}$ MeV, and $\Gamma_{\rm sf} = 4$ MeV;
(2) the scissors mode: $\sigma_{\rm sc} = 10^{-2}|\beta_2|A^{9/10}$ mb, $E_{\rm sc} = 5 \times A^{-1/10}$ MeV, and $\Gamma_{\rm sc} = 1.5$ MeV;
(3) the upbend: $\eta = 0.8$ and $C = 3.5 \times 10^{-8} \exp(-6\beta_2)$ MeV^{-3}.

where the final amplitude of the spin-flip and scissors mode strength has been globally tuned on ARC and NRF data as shown in Figs. 5 and 6, respectively. Globally, the $M1$ strength is properly described except in the transitional region of $A = 180$–190 where the SMLO model overpredicts by a factor of 2 the scissors mode. This overprediction is related to the precise determination of the deformation of these nuclei.

We compare in Fig. 7 the experimental $M1$ photoabsorption cross section of the slightly deformed ^{128}Xe and spherical ^{134}Xe obtained with quasimonoenergetic and linearly polarized γ-ray beams [47] with the D1M + QRPA predictions as well as our new SMLO prescription. Although the SMLO $M1$ cross section in the energy region of the spin-flip resonance is underestimated for both ^{128}Xe and ^{134}Xe, the overall strength is captured. As seen in Fig. 7, the SMLO width for the spin-flip mode is assumed to be constant and, in particular, A-independent, in contrast to what is found with the D1M + QRPA calculation and seen experimentally.

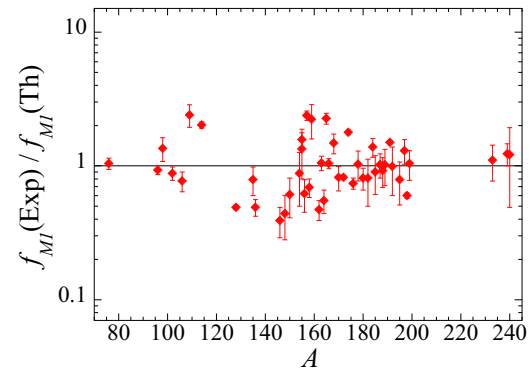

FIG. 5. Comparison between the experimental $M1$ strengths from the ARC data [39] with the SMLO expression [Eq. (7)] predictions for the 47 nuclei recently reanalyzed.

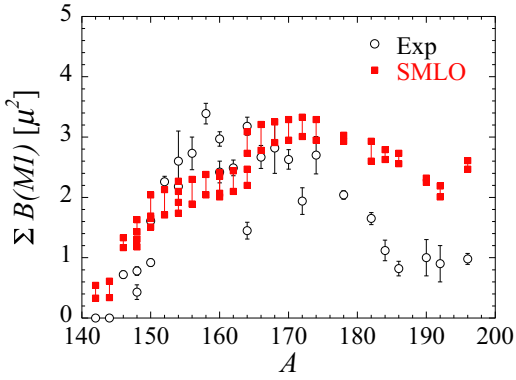

FIG. 6. Comparison between experimental [44] and theoretical (SMLO, full squares) integrated strength $\sum B(M1)(\mu_N^2)$ in the well-defined energy range given by the measurements. The error bars on theoretical values correspond to different estimates of the quadrupole deformation β_2 [41,45,46].

IV. COMPARISON WITH EXPERIMENTS

So far, as described in the previous sections, the $E1$ and $M1$ strength functions obtained within the SMLO model have been tuned on measurements which are almost exclusively sensitive to the specific radiative mode studied. A number of additional experimental data concern the total dipole strength for which it remains difficult to disentangle the $E1$ from the $M1$ components and include the large compilation of average radiative width as well as Oslo data and neutron capture cross sections.

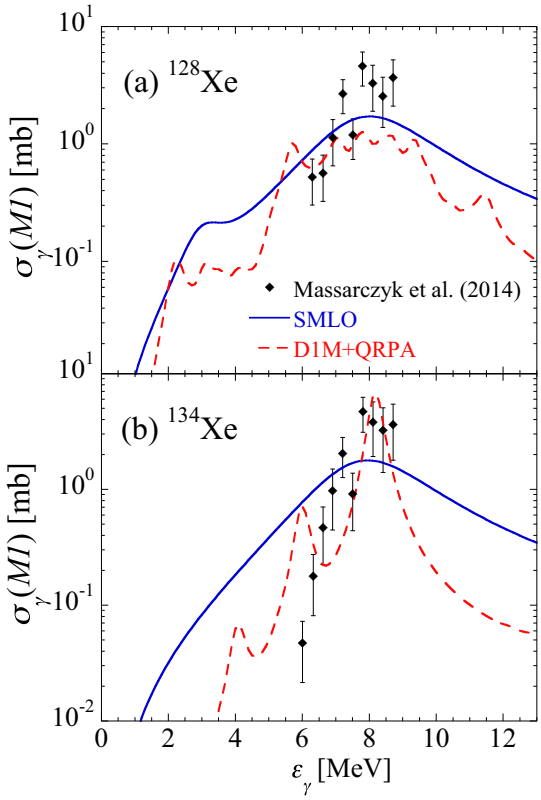

FIG. 7. Comparison among experimental, D1M + QRPA, and SMLO $M1$ strength functions for the $M1$ photoabsorption cross section σ_γ of (a) ^{128}Xe and (b) ^{134}Xe. Experimental data are taken from Ref. [47].

The total $E1 + M1$ SMLO dipole strength is compared with experimental data extracted from the Oslo method in Fig. 8 for 30 nuclei for which Oslo data is available [48]. Note that the dipole strength data extracted from the Oslo method only include experimental systematic uncertainties and not model-dependent statistical uncertainties which can be significantly larger and even change the slope of the dipole strength (see Refs. [49,50] for more details). The low-energy tail of the dipole strength is seen to be globally fairly well reproduced.

Although the upbend does not impact ARC or NRF data, it plays an important role in the estimate of the average radiative width for which many experimental data are available. The average radiative width is defined as [3]

$$\langle\Gamma_\gamma\rangle = \frac{D_0}{2\pi}\sum_{X,L,J,\pi}\int_0^{S_n+E_n} T_{XL}(\varepsilon_\gamma) \times \rho(S_n + E_n - \varepsilon_\gamma, J, \pi)d\varepsilon_\gamma, \quad (9)$$

where D_0 is the average resonance spacing for s-wave neutrons, S_n is the neutron separation energy, E_n is the neutron incident energy, $T_{XL} = 2\pi\varepsilon_\gamma^{2L+1}\overleftarrow{f_{XL}}(\varepsilon_\gamma)$ is the electromagnetic transmission coefficient ($X = M$ or E) for a multipolarity L and ρ is the energy-, spin- (J-), and parity- (π-) dependent nuclear level density.

It has been a long-standing problem that phenomenological SLO models for the $E1$ strength tend to overestimate the average radiative width significantly, whereas its improved and widely used version, the so-called GLO model [18], underestimates $\langle\Gamma_\gamma\rangle$. Such deviations can be found in Ref. [9]. In Fig. 9, we compare the 223 experimental average radiative widths with the SMLO predictions. The low-energy $M1$ components, i.e., the scissors and upbend modes, contribute in a non-negligible way to the $\langle\Gamma_\gamma\rangle$ integral [Eq. (9)] but are not taken into account in the traditional Lorentzian approach [3,18]; this explains why the GLO model underestimates the experimental $\langle\Gamma_\gamma\rangle$. Our new SMLO prescription is found to be globally in agreement with experimental data as shown in Fig. 9 and seen from the root-mean-square (rms) deviations given in Table I.

The deviation with respect to experimental data can be characterized by the $\varepsilon_{\rm rms}$ and $f_{\rm rms}$ factors defined as

$$\varepsilon_{\rm rms} = \exp\left[\frac{1}{N_e}\sum_{i=1}^{N_e}\ln r^i\right], \quad (10)$$

$$f_{\rm rms} = \exp\left[\frac{1}{N_e}\sum_{i=1}^{N_e}\ln^2 r^i\right]^{1/2}, \quad (11)$$

where N_e is the number of experimental data and r^i is, for each data point i, the ratio of theoretical to experimental $\langle\Gamma_\gamma\rangle$ which takes into account the experimental uncertainties $\delta_{\rm exp}$ (see Ref. [9] for more details). We give in Table I the $\varepsilon_{\rm rms}$ and $f_{\rm rms}$ factors for the $\langle\Gamma_\gamma\rangle$ values with

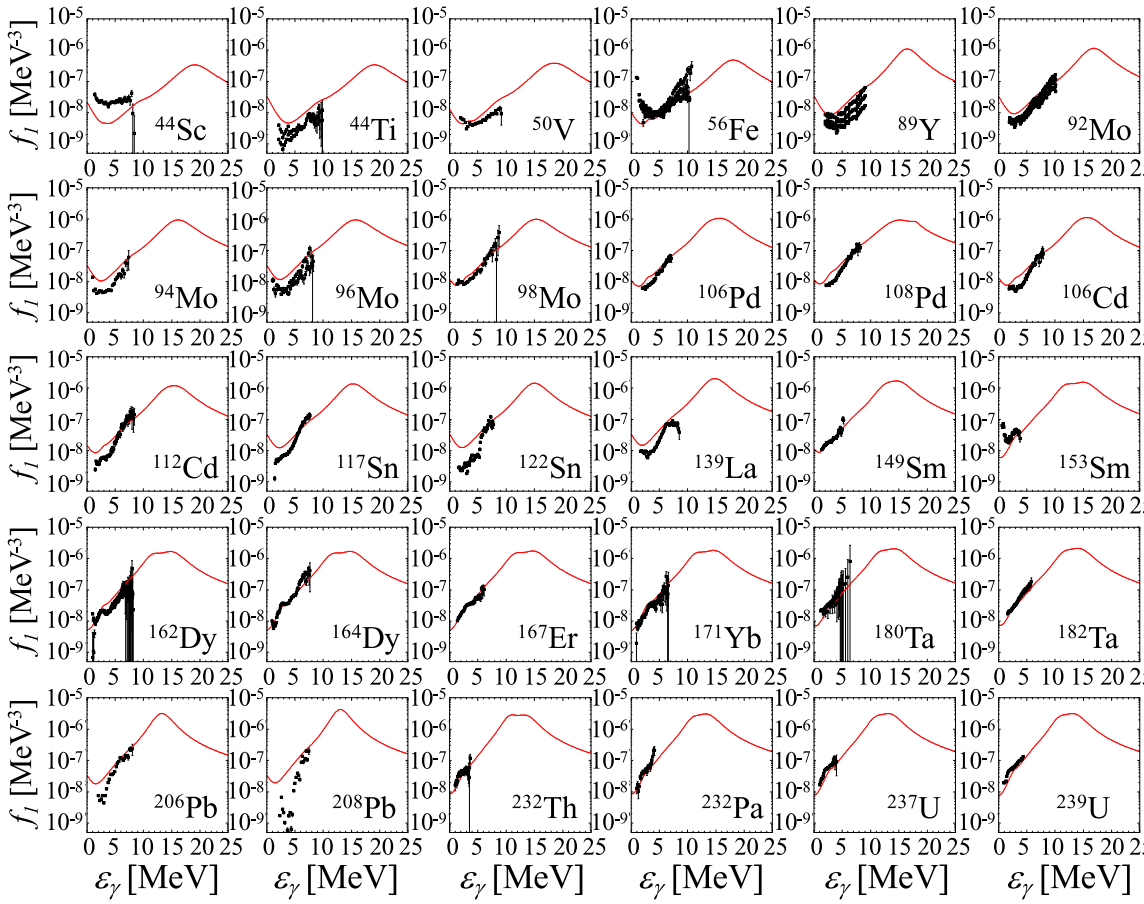

FIG. 8. Comparison of the experimental Oslo strength [48] (black squares) with the SMLO predictions (full red lines) for 30 nuclei between ^{44}Sc and ^{239}U.

respect to the 223 experimental data [3]. Although the RIPL-3 recommended strength clearly gives large deviations, our new SMLO prescriptions reproduce rather well the global trend in a way similar to what is obtained with the D1M + QRPA + 0 lim$^+$ strength [9]. The average radiative width remains however sensitive to the nuclear level densities [see Eq. (9)] as illustrated in Fig. 9 where the error bars on the predictions represent the corresponding sensitivity using different nuclear level-density models [51,52]. As already found in Ref. [9], the constant-temperature level-density formula leads systematically to lower predictions of the average

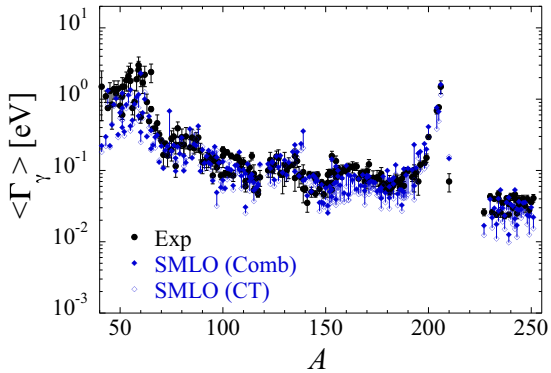

FIG. 9. Comparison between the 223 experimental (black circles) [3] and theoretical (colored diamonds) average radiative width $\langle\Gamma_\gamma\rangle$ as a function of A. The strength corresponds to the SMLO model for the $E1$ and $M1$ including not only the spin flip, but also the scissors and upbend modes. The nuclear level density adopted here is from the combinatorial model [(Comb); blue full diamonds] [51] or the constant temperature [(CT); open blue diamonds] [52].

TABLE I. $\varepsilon_{\rm rms}$ and $f_{\rm rms}$ for the theoretical to experimental ratios of both the $\langle\Gamma_\gamma\rangle$ and the Maxwellian-averaged neutron capture cross sections (MACSs) $\langle\sigma\rangle$. Theoretical estimates are obtained with the present SMLO model, the D1M + QRPA + 0 lim$^+$ [9], and the RIPL-3 recommended strengths [3,18]. Both the CT [52] or the HFB + Comb [51] models of nuclear level densities are considered.

	$\langle\Gamma_\gamma\rangle$		$\langle\sigma\rangle$	
	$\varepsilon_{\rm rms}$	$f_{\rm rms}$	$\varepsilon_{\rm rms}$	$f_{\rm rms}$
SMLO (Comb)	0.90	1.45	1.11	1.47
SMLO (CT)	0.74	1.62	0.98	1.40
D1M + QRPA + 0 lim$^+$ (Comb)	1.02	1.27	1.30	1.55
D1M + QRPA + 0 lim$^+$ (CT)	0.90	1.32	1.15	1.40
RIPL-3 (Comb)	0.48	2.44	0.61	1.92
RIPL-3 (CT)	0.38	3.02	0.53	2.07

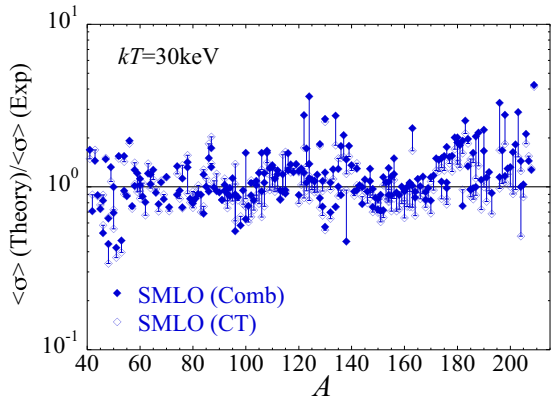

FIG. 10. Ratio of the theoretical to experimental MACS at $kT = 30$ keV as a function of the atomic mass A for all nuclei between Ca and Bi for which experimental MACS exist [54]. The theoretical MACS are obtained with the present SMLO model for the $E1$ and $M1$ strengths. The full symbols are calculations with the HFB + combinatorial model of nuclear level densities [51] and the open symbols with the CT plus Fermi gas model [52].

radiative width in comparison with the HFB + combinatorial model.

The radiative neutron capture cross sections and reaction rates of astrophysical interest have also been calculated systematically on the basis of the Hauser-Feshbach statistical model described by the TALYS reaction code [53]. Figure 10 compares the 240 experimental MACSs [54] at 30 keV for nuclei with $20 \leqslant Z \leqslant 83$ with the TALYS predictions obtained with the present SMLO model. Both the HFB + combinatorial and constant temperature models of nuclear level densities are considered. Note that in the TALYS calculation the strength function is not renormalized as to reproduce the experimental average radiative width. Only nuclei with $Z \geqslant 20$ are considered in the comparison to ensure the validity of the Hauser-Feshbach approach, the cross section for lighter nuclei being affected by the direct contribution [2] and the resolved resonance regime [55] at the 30-keV neutron energies considered here. The deviation with respect to experimental data can be characterized by the same $\varepsilon_{\rm rms}$ and $f_{\rm rms}$ factors as defined for the average radiative width [Eqs. (10) and (11)], this time with the ratio $r^i = \langle\sigma\rangle^i_{\rm th}/\langle\sigma\rangle^i_{\rm exp}$. As shown in Table I, the rms deviation factors are quite satisfactory with the SMLO prescription, relatively comparable to those obtained with D1M + QRPA + 0 lim$^+$ and significantly better than with the former RIPL-3 recommendation, for which an $f_{\rm rms}$ deviation of about 2 and mean deviation $\varepsilon_{\rm rms} \simeq 0.5$ are obtained. The MACS as well as the average radiative widths are clearly underestimated by the former RIPL-3 prescriptions. This explains the need to renormalize the average radiative width on experimental data to reproduce properly the radiative neutron capture cross section. This long-standing problem is largely solved with the present updated SMLO prescriptions where both the average radiative width and the neutron capture cross sections are consistently estimated and globally in agreement with experimental data. Such a conclusion holds regardless of the nuclear level-density model adopted.

V. CONCLUSIONS

Valuable theoretical predictions of nuclear dipole excitations in the whole chart of nuclei are of great interest for different nuclear applications, including, in particular, nuclear astrophysics. Here on the basis of experimental and theoretical information on the $E1$ and $M1$ strength functions, inspired both from axially deformed QRPA and from SM calculations, we derive simple expressions to determine systematically the dipole strength in order to update former prescriptions with a special emphasis on new expressions for both the spin-flip and the scissors mode components of the $M1$ strength. Such expressions present the advantage of being easily tuned on experimental data but also adjustable to reproduce measured cross sections. We have extended our prescriptions of the photoabsorption strength to the determination of the deexcitation strength function by adding a temperature dependence to the $E1$ GDR width and an $M1$ upbend at the lowest energies. This extra strength together with the scissors mode impact the overall radiative width as well as the radiative neutron capture cross section, especially due to the increasing $M1$ strength at decreasing photon energies. We compared our SMLO $E1$ and $M1$ strengths with available experimental data at low energies and show that a relatively good agreement is obtained. Finally, note that the expressions are kept as simple as possible, still trying to capture as much as possible the microscopic QRPA and SM patterns. If more sophisticated functionals are required, it is then suggested to consider rather the fully microscopic predictions, such as the tabulated $E1$ and $M1$ D1M + QRPA strength [9]. In the meantime, the new expressions are believed to be more precise and more physical than most of the analytical systematics proposed in the past, such as the recommended RIPL-3 prescriptions [3].

ACKNOWLEDGMENTS

S.G. acknowledges support from the FRS-FNRS. This work was performed within the IAEA CRP on "Updating the Photonuclear Data Library and generating a Reference Database for Photon Strength Functions" (Project No. F410 32). The authors also thank J. Kopecky for providing updated ARC data and O. Gorbachenko for fruitful discussions.

[1] M. Arnould, S. Goriely, and K. Takahashi, Phys. Rep. **450**, 97 (2007).

[2] Y. Xu, S. Goriely, A. J. Koning, and S. Hilaire, Phys. Rev. C **90**, 024604 (2014).

[3] R. Capote, M. Herman, P. Oblozinsky, P. Young, S. Goriely, T. Belgya, A. Ignatyuk, A. Koning, S. Hilaire, V. Plujko, M. Avrigeanu, O. Bersillon *et al.*, Nucl. Data Sheets **110**, 3107 (2009).

[4] S. Goriely and E. Khan, Nucl. Phys. A **706**, 217 (2002).
[5] S. Goriely, E. Khan, and M. Samyn, Nucl. Phys. A **739**, 331 (2004).
[6] I. Daoutidis and S. Goriely, Phys. Rev. C **86**, 034328 (2012).
[7] M. Martini, S. Péru, S. Hilaire, S. Goriely, and F. Lechaftois, Phys. Rev. C **94**, 014304 (2016).
[8] S. Goriely, S. Hilaire, S. Péru, M. Martini, I. Deloncle, and F. Lechaftois, Phys. Rev. C **94**, 044306 (2016).
[9] S. Goriely, S. Hilaire, S. Péru, and K.Sieja, Phys. Rev. C **98**, 014327 (2018).
[10] G. Colò and P. Bortignon, Nucl. Phys. A **696**, 427 (2001).
[11] D. Sarchi, P. Bortignon, and G. Colò, Phys. Lett. B **601**, 27 (2004).
[12] N. Tsoneva and H. Lenske, Phys. Rev. C **77**, 024321 (2008).
[13] P. Papakonstantinou and R. Roth, Phys. Lett. B **671**, 356 (2009).
[14] O. Achakovskiy, A. Avdeenkov, S. Goriely, S. Kamerdzhiev, and S. Krewald, Phys. Rev. C **91**, 034620 (2015).
[15] D. Gambacurta, M. Grasso, and O. Vasseur, Phys. Lett. B **777**, 163 (2018).
[16] E. Litvinova, P. Ring, and V. Tselyaev, Phys. Rev. C **88**, 044320 (2013).
[17] I. A. Egorova and E. Litvinova, Phys. Rev. C **94**, 034322 (2016).
[18] J. Kopecky and M. Uhl, Phys. Rev. C **41**, 1941 (1990).
[19] D. Brink, Ph.D. thesis, University of Oxford, 1955.
[20] P. Axel, Phys. Rev. **126**, 671 (1962).
[21] V. Plujko, R. Capote, and O. Gorbachenko, At. Data Nucl. Data Tables **97**, 567 (2011).
[22] V. Plujko, O. Gorbachenko, R. Capote, and P. Dimitriou, At. Data Nucl. Data Tables **123**, 1 (2018).
[23] G. Schramm, R. Massarczyk, A. R. Junghans, T. Belgya, R. Beyer, E. Birgersson, E. Grosse, M. Kempe, Z. Kis, K. Kosev, M. Krtička, A. Matic *et al.*, Phys. Rev. C **85**, 014311 (2012).
[24] M. R. Mumpower, T. Kawano, J. L. Ullmann, M. Krtička, and T. M. Sprouse, Phys. Rev. C **96**, 024612 (2017).
[25] E. Grosse, A. Junghans, and R. Massarczyk, Eur. Phys. J. A **53**, 225 (2017).
[26] A. Voinov, E. Algin, U. Agvaanluvsan, T. Belgya, R. Chankova, M. Guttormsen, G. E. Mitchell, J. Rekstad, A. Schiller, and S. Siem, Phys. Rev. Lett. **93**, 142504 (2004).
[27] M. Guttormsen, R. Chankova, U. Agvaanluvsan, E. Algin, L. A. Bernstein, F. Ingebretsen, T. Lönnroth, S. Messelt, G. E. Mitchell, J. Rekstad, A. Schiller, S. Siem *et al.*, Phys. Rev. C **71**, 044307 (2005).
[28] R. Schwengner, S. Frauendorf, and A. C. Larsen, Phys. Rev. Lett. **111**, 232504 (2013).
[29] B. A. Brown and A. C. Larsen, Phys. Rev. Lett. **113**, 252502 (2014).
[30] K. Sieja, Phys. Rev. Lett. **119**, 052502 (2017).
[31] K. Sieja, EPJ Web Conf. **146**, 05004 (2017).
[32] S. Karampagia, B. A. Brown, and V. Zelevinsky, Phys. Rev. C **95**, 024322 (2017).
[33] R. Schwengner, S. Frauendorf, and B. A. Brown, Phys. Rev. Lett. **118**, 092502 (2017).
[34] W. Myers, W. Swiatecki, T. Kodama, L. J. El-Jaick, and E. R. Hilf, Phys. Rev. C **15**, 2032 (1977).
[35] E. Lipparini and S. Stringari, Phys. Rep. **175**, 103 (1989).
[36] O. Bohigas, A. Lane, and J. Martorell, Phys. Rep. **51**, 267 (1979).
[37] P. Gleissl, M. Brack, J. Meyer, and P. Quentin, Ann. Phys. (N.Y.) **197**, 205 (1990).
[38] V. A. Plujko, I. M. Kadenko, E. V. Kulich, S. Goriely, O. I. Davidovskaya, and O. M. Gorbachenko, in *Workshop on Photon Strength Functions and Related Topics, Prague, Czech Republic, 2007*, edited by F. Becvar (SISSA, Trieste, Italy, 2007), Vol. 002.
[39] J. Kopecky, S. Goriely, S. Péru, S. Hilaire, and M. Martini, Phys. Rev. C **95**, 054317 (2017).
[40] K. Heyde, P. von Neumann-Cosel, and A. Richter, Rev. Mod. Phys. **82**, 2365 (2010).
[41] S. Goriely, S. Hilaire, M. Girod, and S. Péru, Phys. Rev. Lett. **102**, 242501 (2009).
[42] J. E. Midtbø, A. C. Larsen, T. Renstrøm, F. L. B. Garrote, and E. Lima, Phys. Rev. C **98**, 064321 (2018).
[43] M. Krtička, S. Goriely, S. Hilaire, and S. Péru, Phys. Rev. C (unpublished).
[44] N. Pietralla, P. von Brentano, R.-D. Herzberg, U. Kneissl, N. Lo Iudice, H. Maser, H. H. Pitz, and A. Zilges, Phys. Rev. C **58**, 184 (1998).
[45] S. Goriely, N. Chamel, and J. M. Pearson, Phys. Rev. C **88**, 061302(R) (2013).
[46] P. Möller, A. Sierk, T. Ichikawa, and H. Sagawa, At. Data Nucl. Data Tables **109-110**, 1 (2016).
[47] R. Massarczyk, G. Rusev, R. Schwengner, F. Dönau, C. Bhatia, M. E. Gooden, J. H. Kelley, A. P. Tonchev, and W. Tornow, Phys. Rev. C **90**, 054310 (2014).
[48] Oslo database, Level Densities and Gamma-Ray Strength Functions (2017) [http://www.mn.uio.no/fysikk/english/research/about/infrastructure/OCL/nuclear-physics-research/compilation/].
[49] H. Utsunomiya, S. Goriely, T. Kondo, C. Iwamoto, H. Akimune, T. Yamagata, H. Toyokawa, H. Harada, F. Kitatani, Y.-W. Lui, A. Larsen, M. Guttormsen *et al.*, Phys. Rev. C **88**, 015805 (2013).
[50] B. V. Kheswa, M. Wiedeking, J. A. Brown, A. C. Larsen, S. Goriely, M. Guttormsen, F. L. B. Garrote, L. A. Bernstein, D. L. Bleuel, T. K. Eriksen, F. Giacoppo, A. Gorgen *et al.*, Phys. Rev. C **95**, 045805 (2017).
[51] S. Goriely, S. Hilaire, and A. J. Koning, Phys. Rev. C **78**, 064307 (2008).
[52] A. J. Koning, S. Hilaire, and S. Goriely, Nucl. Phys. A **810**, 13 (2008).
[53] A. J. Koning and D. Rochman, Nucl. Data Sheets **113**, 2841 (2012)
[54] I. Dillmann, M. Heil, F. Käppeler, R. Plag, T. Rauscher, and F.-K. Thielemann, in *Capture Gamma-Ray Spectroscopy and Related Topics: 12th International Symposium*, edited by A. Woehr and A. Aprahamian, AIP Proc. No. 819 (AIP, New York, 2006), p. 123.
[55] D. Rochman, S. Goriely, A. Koning, and H. Ferroukhi, Phys. Lett. B **764**, 109 (2017).

Correction: A global misspelling was introduced during the production process and has been fixed.